A fast numerical method for computing the linear and nonlinear mechanical properties of composites

H. Moulinec, Pierre Suquet

Mécanique des solides/*Mechanics of Solids*

A fast numerical method for computing the linear and nonlinear mechanical properties of composites

Hervé Moulinec and Pierre Suquet

Abstract – This Note is devoted to a new iterative algorithm to compute the local and overall response of a composite from images of its (complex) microstructure. The elastic problem for a heterogeneous material is formulated with the help of a homogeneous reference medium and written under the form of a periodic Lippman-Schwinger equation. Using the fact that the Green's function of the pertinent operator is known explicitly in Fourier space, this equation is solved iteratively. The method is extended to the case where the individual constituents are elastic-plastic Von Mises materials with isotropic hardening.

Une méthode de calcul rapide des propriétés macroscopiques linéaires et non linéaires de composites

Résumé – *Cette Note est consacrée à un nouvel algorithme de détermination de la réponse locale et du comportement global d'un composite, à partir d'images complexes de sa microstructure. Le problème d'une hétérogénéité élastique est tout d'abord reformulé à l'aide d'un milieu homogène de référence ce qui conduit à une équation de Lippman-Schwinger périodique, Cette équation, dont la fonction de Green est explicitement connue dans l'espace de Fourier, est résolue itérativement. L'algorithme proposé est étendu à des phases présentant un comportement élasto-plastique avec écrouissage.*

Version française abrégée – Le but de cette étude est de développer une méthode de simulation numérique du comportement d'un matériau hétérogène à partir d'images réelles ou de simulations morphologiques de sa micro-structure. La richesse de description requise et le nombre élevé de pixels, et donc d'inconnues en jeu, écartent la méthode des éléments finis. Un algorithme itératif de résolution du problème local utilisant les transformées de Fourier discrètes de l'image et des champs de contraintes et de déformation est proposé et mis en œuvre dans le cas d'un comportement linéaire et d'un comportement non linéaire des constituants.

La détermination des caractéristiques élastiques d'un matériau composite repose sur la définition d'un volume élémentaire représentatif V et la résolution du problème local sur V,

$$(1) \quad \begin{cases} \sigma(\mathbf{x}) = \mathbf{c}(\mathbf{x}) : (\epsilon(\mathbf{u}^*(\mathbf{x})) + \mathbf{E}) & \text{dans V,} \\ \operatorname{div}(\sigma) = 0 & \text{dans V,} \quad \mathbf{u}^*\#, \quad \sigma \cdot \mathbf{n} - \#. \end{cases}$$

$\mathbf{c}(\mathbf{x})$ est le tenseur d'élasticité du matériau dont la donnée est disponible sous forme d'une image, chaque pixel pouvant correspondre à un matériau différent. Le problème est « fermé » par des conditions aux limites de périodicité (faute de connaître la micro-structure réelle en dehors de l'image) et les notations $\mathbf{u}^*\#$, $\sigma \cdot \mathbf{n} - \#$ désignent un champ périodique $\mathbf{u}^*$ et un champ anti-périodique $\sigma \cdot \mathbf{n}$. En introduisant un matériau de référence, élastique, homogène de tenseur d'élasticité $\mathbf{c}^0$, et le tenseur de Green périodique Γ^0 de l'opérateur élastique associé à ce matériau de référence, (1) équivaut à l'équation de Lippman-Schwinger périodique, qui s'écrit dans l'espace réel et dans l'espace de Fourier:

$$(4) \quad \begin{cases} \epsilon(\mathbf{u}) = -\Gamma^0 \star (\delta\mathbf{c} : \epsilon(\mathbf{u})) + \mathbf{E}, \\ \hat{\epsilon}(\xi) = -\hat{\Gamma}^0(\xi) : \widehat{\delta\mathbf{c} : \epsilon}(\xi) \quad \forall \xi \neq 0, \quad \hat{\epsilon}(0) = \mathbf{E} \end{cases}$$

L'équation (4) est résolue par un algorithme itératif (présenté en (5) ci-dessous) permettant de déterminer la valeur des contraintes et des déformations en un nombre $N \times N$ discret de

---

points, régulièrement espacés, de la cellule de base. Cet algorithme contient une étape dans l'espace réel (pour le calcul de $\delta c : \epsilon(u)$) et une étape dans l'espace de Fourier (pour le calcul de $\Gamma^0 \star (\delta c : \epsilon(u))$), le passage d'un espace à l'autre étant assuré par la transformée de Fourier et son inverse.

Cet algorithme de résolution du problème d'élasticité linéaire peut être utilisé pour résoudre des problèmes non linéaires, en formulation sécante ou incrémentale. L'algorithme (8) proposé plus loin couvre le cas de la plasticité incrémentale avec ou sans écrouissage. Cette méthode a été mise en œuvre en dimension 2 sur des configurations modèles de disques de rayons identiques dont les centres sont tirés aléatoirement dans une cellule carrée, sous la seule condition de non interpénétrabilité. Les essais numériques effectués mettent en évidence que les résultats peuvent être sensibles à la résolution de l'image dans le cas d'un comportement non linéaire (comme la plasticité parfaite) tandis qu'ils sont peu affectés par cette résolution dans le cas du comportement élastique linéaire. L'examen de 10 tirages aléatoires de 64 fibres dans une cellule carrée, permet entre autres de juger de la représentativité des calculs classiques effectués sur une cellule de base hexagonale ou carrée contenant une fibre unique. On montre que la moyenne des propriétés élastiques des configurations aléatoires est correctement approchée par le calcul sur cellule hexagonale. En revanche, pour une matrice à écrouissage linéaire, ce même calcul sous estime de façon significative la réponse moyenne des configurations aléatoires.

The aim of this Note is to present a numerical method for the determination of the overall and local response of a composite material from actual images or morphological simulations of its microstructure. The large number of unknowns involved in the problem prohibits the choice of commonly used algorithms based on the Finite Element Method. An iterative algorithm making use of the Fourier transform of the stress and strain fields is proposed and applied to composite materials with local nonlinear behavior.

1. THE PERIODIC LIPPMAN-SCHWINGER EQUATION. – The determination of the effective elastic properties of a composite requires the definition of a representative volume element V and the resolution of a local problem on V,

$$(1) \qquad \sigma(x) = c(x) : \epsilon(u(x)) \quad \text{in } V, \qquad \operatorname{div}(\sigma) = 0 \quad \text{in } V.$$

$c(x)$ is the stiffness tensor of the material and it may be determined from an image of the microstructure which can vary from one pixel to another. The local strain field $\epsilon(u(x))$ can be split into its average E, which is prescribed, and a fluctuation term $\epsilon(u^*(x))$ which is unknown:

$$\epsilon(u(x)) = \epsilon(u^*(x)) + E, \qquad \langle \epsilon(u) \rangle = E.$$

Here $\langle \cdot \rangle$ denotes the spatial average over V. In the absence of information about the microstructure outside the image, several conditions can be imposed on the boundary of V. Our choice is to close (1) with the periodic boundary conditions:

$$(2) \qquad\qquad\qquad u^* \#, \qquad \sigma \cdot n - \#,$$

where the notations $u^* \#$ and $\sigma \cdot n - \#$ denote a periodic and an anti-periodic field, respectively.

A linear-elastic reference material, which is homogeneous and isotropic with stiffness tensor $\mathbf{c}^0$ is introduced. Problem (1) can then be alternatively written:

$$(3) \quad \begin{cases} \sigma(\mathbf{x}) = \mathbf{c}^0 : (\epsilon(\mathbf{u}^*(\mathbf{x})) + \mathbf{E}) + \tau(\mathbf{x}), \\ \mathbf{div}(\sigma) = \mathbf{0} \quad \text{in } V, \qquad \mathbf{u}^*\#, \quad \sigma \cdot \mathbf{n} - \#, \end{cases}$$

where $\tau = \delta\mathbf{c} : (\epsilon(\mathbf{u}^*) + \mathbf{E})$ is unknown *a priori* $(\delta\mathbf{c}(\mathbf{x}) = \mathbf{c}(\mathbf{x}) - \mathbf{c}^0)$. The solution of (3) can be expressed in real and Fourier spaces, respectively, by means of the periodic Green operator $\mathbf{\Gamma}^0$ associated with the homogeneous elastic tensor $\mathbf{c}^0$:

$$\epsilon(\mathbf{u})(\mathbf{x}) = -\mathbf{\Gamma}^0(\mathbf{x}) \star \tau(\mathbf{x}) + \mathbf{E};$$

$$\hat{\epsilon}(\boldsymbol{\xi}) = -\hat{\mathbf{\Gamma}}^0(\boldsymbol{\xi}) : \hat{\tau}(\boldsymbol{\xi}) \qquad \forall \boldsymbol{\xi} \neq \mathbf{0}, \quad \hat{\epsilon}(\mathbf{0}) = \mathbf{E}.$$

The solution of (1) therefore reduces to the solution of the *periodic Lippman-Schwinger equation* (Kröner, 1972), which reads, in real space and in Fourier space, respectively:

$$(4) \quad \begin{cases} \epsilon(\mathbf{u}) = -\mathbf{\Gamma}^0 \star (\delta\mathbf{c} : \epsilon(\mathbf{u})) + \mathbf{E}, \\ \hat{\epsilon}(\boldsymbol{\xi}) = -\hat{\mathbf{\Gamma}}^0(\boldsymbol{\xi}) : \widehat{(\delta\mathbf{c}:\epsilon)}(\boldsymbol{\xi}) \qquad \forall \boldsymbol{\xi} \neq \mathbf{0}, \qquad \hat{\epsilon}(\mathbf{0}) = \mathbf{E} \end{cases}$$

The algorithm. – Equation (4) is solved by means of the iterative algorithm:

$$(5) \quad \begin{cases} \textit{Initialization}: \quad \epsilon^0(\mathbf{x}) = \mathbf{E}, \qquad \forall \mathbf{x} \in V, \\ \textit{Iteration } i+1: \quad \epsilon^i \text{ is known} \\ a)\ \sigma^i = \mathbf{c} : \epsilon^i. \text{ Convergence test.} \\ b)\ \tau^i = \sigma^i - \mathbf{c}^0 : \epsilon^i, \\ c)\ \hat{\tau}^i = \mathcal{F}(\tau^i), \\ d)\ \hat{\epsilon}^{i+1}(\boldsymbol{\xi}) = -\hat{\mathbf{\Gamma}}^0(\boldsymbol{\xi}) : \hat{\tau}^i(\boldsymbol{\xi}) \qquad \forall \boldsymbol{\xi} \neq \mathbf{0} \text{ and } \hat{\epsilon}^{i+1}(\mathbf{0}) = \mathbf{E}, \\ e)\ \epsilon^{i+1} = \mathcal{F}^{-1}(\hat{\epsilon}^{i+1}) \end{cases}$$

where $\mathcal{F}$ and $\mathcal{F}^{-1}$ denote the Fourier transform and its inverse, respectively:

Convergence test. – The iterative process is stopped when the error e

$$(6) \quad e = \frac{(\langle \|\mathrm{div}(\sigma^i)\|^2 \rangle)^{1/2}}{\|\Sigma^i\|} = \frac{(\langle \|\boldsymbol{\xi} \cdot \hat{\sigma}^i\|^2 \rangle)^{1/2}}{\|\hat{\sigma}^i(\mathbf{0})\|^2}$$

is less than the desired precision (typically of the order of 10^{-4}).

Choice of the reference medium. – The operator $\mathbf{\Gamma}^0$ is known explicitly in Fourier space. For example, when the reference material is isotropic, it takes the form (Suquet, 1990):

$$\hat{\Gamma}^0_{khij}(\boldsymbol{\xi}) = \frac{1}{4\,\mu^0\,|\boldsymbol{\xi}|^2} (\delta_{ki}\,\xi_h\,\xi_j + \delta_{hi}\,\xi_k\,\xi_j + \delta_{kj}\,\xi_h\,\xi_i + \delta_{hj}\,\xi_k\,\xi_i)$$

$$- \frac{\lambda^0 + \mu^0}{\mu^0(\lambda^0 + 2\mu^0)} \frac{\xi_i\,\xi_j\,\xi_k\,\xi_h}{|\boldsymbol{\xi}|^4}.$$

typo in the original version: a factor 2 was missing (HM 3-Nov-2020)

The rate of convergence of the algorithm is governed by the choice of the Lamé coefficients λ^0, μ^0 of the reference medium. For a two-phase composite material the best convergence rate was observed when these coefficients were prescribed to be the half sum of the Lamé coefficients of each phase.

2. NONLINEAR BEHAVIOR. – The above-described procedure has been extended to the case where the individual constituents exhibit nonlinear elastic-plastic behavior of the flow theory type. This extension follows a scheme of integration which is standard in the context of applications of the FEM to elastic-plastic structures. For simplicity, in the sequel, attention will be restricted to Von Mises materials with isotropic hardening:

$$(7) \qquad \dot{\boldsymbol{\sigma}} = \mathbf{c} : (\dot{\boldsymbol{\epsilon}} - \dot{\boldsymbol{\epsilon}}^p), \qquad \dot{\boldsymbol{\epsilon}}^p = \dot{p}\,\frac{3}{2}\,\frac{\mathbf{s}}{\sigma_{\mathrm{eq}}}, \qquad \sigma_{\mathrm{eq}} - \sigma_0\,(p) \leqq 0, \qquad \dot{p} \geqq 0.$$

$\boldsymbol{\epsilon}^p$ denotes the plastic strain tensor, p is the hardening parameter. The time interval (or, alternatively, the loading path) is discretized into subintervals $[t_n,\ t_{n+1}]$. The strain, stress and hardening parameter fields at time t_m, denoted $(\boldsymbol{\epsilon}_m,\ \boldsymbol{\sigma}_m,\ p_m)$, are searched for. Assuming that these values are known at step n (time t_n), the principal unknown at step $n+1$ is $\boldsymbol{\epsilon}_{n+1}$. The incremental equations (7) are discretized by means of an implicit scheme. The unknown $\boldsymbol{\epsilon}_{n+1}$ is a compatible strain field such that the stress field associated to it by the constituve law is in equilibrium (note that the resulting system of equations to be solved for $\boldsymbol{\epsilon}_{n+1}$ is nonlinear). Thus, in summary, the algorithm for the determination of $\boldsymbol{\epsilon}_{n+1}$ is:

$$(8) \quad \left\{ \begin{array}{l} \textit{Iteration } i+1: \quad \boldsymbol{\epsilon}_{n+1}^{i} \text{ is known,} \\[4pt] a)\ \text{Compute } \boldsymbol{\sigma}_{n+1}^{i} \text{ and } p_{n+1}^{i} \text{ from } (\boldsymbol{\epsilon}_{n+1}^{i}, \boldsymbol{\sigma}_n, \boldsymbol{\epsilon}_n, p_n), \\[4pt] \qquad \text{Convergence test,} \\[4pt] b)\ \boldsymbol{\tau}_{n+1}^{i} = \boldsymbol{\sigma}_{n+1}^{i} - \mathbf{c}^0 : \boldsymbol{\epsilon}_{n+1}^{i}, \\[4pt] c)\ \hat{\boldsymbol{\tau}}_{n+1}^{i} = \mathcal{F}(\boldsymbol{\tau}_{n+1}^{i}), \\[4pt] d)\ \hat{\boldsymbol{\epsilon}}_{n+1}^{i+1}(\boldsymbol{\xi}) = -\hat{\boldsymbol{\Gamma}}^0(\boldsymbol{\xi}) : \hat{\boldsymbol{\tau}}_{n+1}^{i}(\boldsymbol{\xi}) \qquad \forall\,\boldsymbol{\xi} \neq \mathbf{0}, \quad \hat{\boldsymbol{\epsilon}}_{n+1}^{i+1}(\mathbf{0}) = \mathbf{E}_{n+1}, \\[4pt] e)\ \boldsymbol{\epsilon}_{n+1}^{i+1} = \mathcal{F}^{-1}(\hat{\boldsymbol{\epsilon}}_{n+1}^{i+1}). \end{array} \right.$$

The computation of $\boldsymbol{\sigma}_{n+1}^{i}$, p_{n+1}^{i} from $(\boldsymbol{\epsilon}_{n+1}^{i}, \boldsymbol{\sigma}_n, \boldsymbol{\epsilon}_n, p_n)$ [step a in algorithm (8)] is performed by means of a radial return method.

3. APPLICATIONS. – The present algorithm has been implemented in dimension 2 under the assumption of generalized plane strain (Michel and Suquet, 1993). An image is discretized into $N \times N$ pixels and the discrete Fourier transform associated with this spatial discretization is used. The sampling of the image has an influence on the accuracy of the results (*see* section 3.1). The method allows to investigate the influence of fibers arrangement on the overall response of a composite reinforced by aligned continuous fibers (*see* section 3.2). The loading consists of a uniaxial tension in the transverse plane (in $0°$ direction for all random configurations). All the calculations were carried out using fibers with identical cross sections at a fixed volume fraction of 0.475. The following material properties were assumed:

$$(9) \quad \left\{ \begin{array}{l} \text{Elastic fibers}: \ \mathrm{E}_f = 400,000\,\mathrm{MPa}, \ \nu_f = 0.23, \\[4pt] \text{Elastic-plastic matrix}: \ \mathrm{E}_m = 68,900\,\mathrm{MPa}, \ \nu_m = 0.35, \ \sigma_0\,(p) = \sigma_0 + \mathrm{H}\,p, \\[4pt] \sigma_0 = 68.9\,\mathrm{MPa}, \ \mathrm{H} = 0 \ (\text{perfect plasticity}) \text{ or } \mathrm{H} = 1,710\,\mathrm{MPa} \ (\text{linear hardening}). \end{array} \right.$$

3.1. *The influence of spatial resolution.* – The spatial resolution of the image, measured by the number N of pixels on each coordinate axis, has a significant influence on the accuracy of the results in the nonlinear range. This accuracy is assessed by comparison

with results obtained on two standard configurations consisting of circular fibers placed at the centers of a square or of a hexagonal unit cell. In the latter case the two unit directions of the lattice are the $\pm 30°$ directions. The images which have been considered contain $N \times N$ pixels with $N = 32$, 64, 128, 256, 512, 1 024. For the purpose of testing the accuracy of the procedure, the results of the calculations at various resolutions were compared with the results at the highest resolution, taken as a reference.

The transverse Young modulus was observed to be rather insensitive to the spatial resolution of the image and did not vary by more than 1% in the range of resolutions investigated. On the other hand the overall hardening modulus, in the case of a matrix with a linear hardening, was observed to vary by 7%, but these variations were less than 3% when N was taken to be larger than 64. The overall property which was observed to be the most sensitive to spatial resolution was the overall flow stress, when the matrix is perfectly plastic. In fact, the deviation can reach 15% for a square unit cell at low resolution. A resolution of at least $N = 128$ is suggested to ensure deviations of less than 5%.

The discrepancy of the results for varying resolutions is related to the strong tendency of the matrix to undergo shear localization. In the perfectly plastic case, discontinuous solutions might appear (shear planes passing through the matrix). Hardening of the matrix inhibits such localization phenomena (at least in the setting of infinitesimal strains considered here). In this latter case, the overall behavior of the composite is stable and is therefore less sensitive to changes in geometrical parameters, in general, and more specifically, to spatial resolution. In addition, the stiff gradients associated with strain localization yield high frequencies in the Fourier transform of the strain field. The spatial sampling required to compute accurately these high-frequency terms increases with the strain localization.
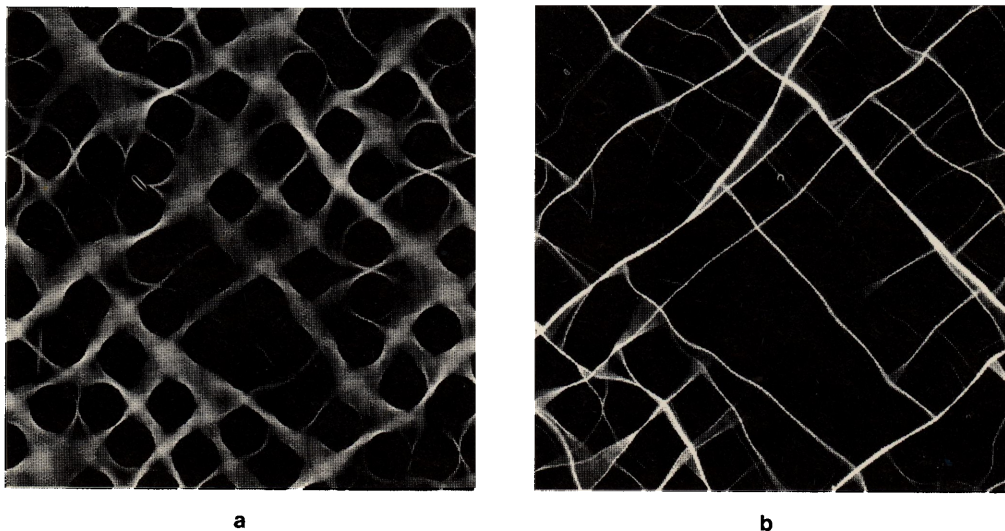

a   b

Fig. 1. – Uniaxial tensile test on a unit cell containing 64 fibers discretized with 1,024 × 1,024 pixels. Volume fraction of fibers = 0.475. Contours of the local equivalent strain for 1% of overall strain in the direction x. Constitutive parameters given in (9). Black: $\varepsilon_{eq}^p = 0\%$, white: $\varepsilon_{eq}^p \geq 10\%$. (a) matrix with linear hardening. (b) perfectly plastic matrix.

Fig. 1. – Traction simple à 0° sur une cellule contenant 64 fibres discrétisée en 1 024 × 1 024 pixels. Fraction volumique de fibres = 0,475. Cartes de la déformation plastique équivalente pour une déformation macroscopique dans la direction x de 1%. Noir: $\varepsilon_{eq}^p = 0\%$, blanc: $\varepsilon_{eq}^p = 10\%$. Paramètres constitutifs donnés par (9). (a) matrice à écrouissage linéaire. (b) matrice parfaitement plastique.

3.2. *The influence of the fibers arrangement in transversely isotropic composites.* – The present method can be used to investigate the influence of the arrangement of the fibers on the effective response of composites reinforced by long fibers subjected to uniaxial transverse stresses. For this purpose fibers with an identical circular cross section are placed at random in the unit cell under the only restriction of non-interpenetrability of the disks. 10 images at a spatial resolution of $1{,}024 \times 1{,}024$ points containing 64 fibers with a constant volume fraction (0.475) are considered. The two other configurations considered are standard in most FEM-based studies of the problem. They consist of single circular fibers placed at the nodes of a square or hexagonal lattice. The results are shown in figure 2. The square array has a marked transverse anisotropy, strengthened by the nonlinear behavior, which gives raise to different responses when the direction of tension makes an angle of $0°$ or $45°$ with one of the axis of the square lattice. The hexagonal lattice, which approaches transverse isotropy, systematically underestimates the stiffness of the composite. A similar observation was made in Nakamura and Suresh (1993) where, however, the hexagonal lattice was considered as isotropic in the nonlinear range.

Transverse Young's modulus. – The deviation of the transverse Young's moduli calculated in the 10 configurations from their average is 0.9%. The hexagonal array gives a value which underestimates this average value by 2%. The square array is anisotropic and the Young's modulus at $0°$ and at $45°$ are respectively 7.5% higher and 9.8% lower than the average of the random configurations.

Hardening modulus. – For the volume fraction under consideration, all the responses of the 10 random cells are located above the predictions for the hexagonal array and in

(a)   (b)
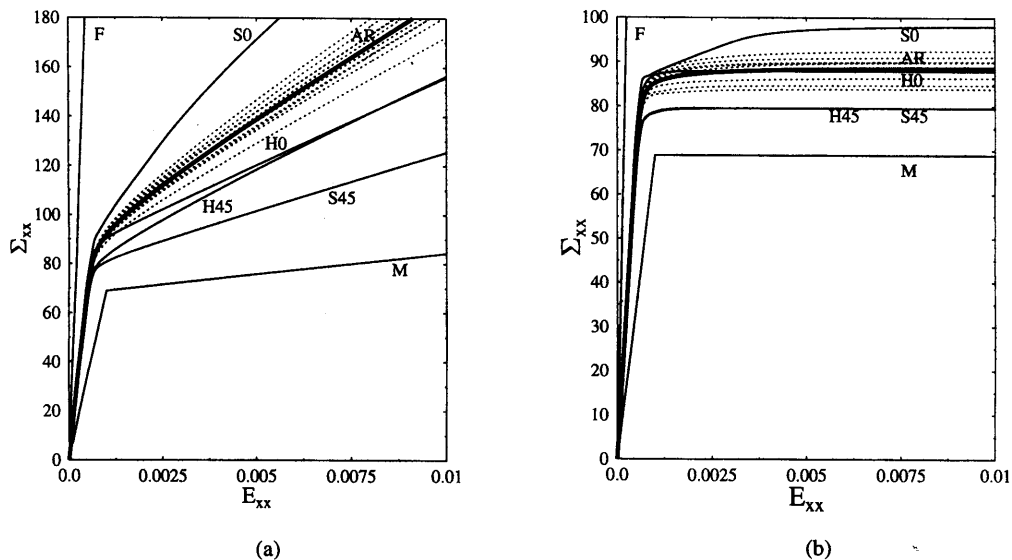
Fig. 2. – Overall stress-strain curves computed with the present method. Volume fraction of fibers = 0.475. Dotted lines: 10 random configurations (circular fibers with identical radii and centers chosen at random). F: fibers. M: matrix. AR: average over the random configurations. S0 (S45): response of the square array containing one circular fiber under a tensile stress applied in a direction making an angle of $0°$ (resp. $45°$) with respect to the x direction. H0 and H45: *idem* for a hexagonal unit cell. (*a*) matrix with linear hardening. (*b*) perfectly plastic matrix.

Fig. 2. – *Courbes contrainte-déformation macroscopiques calculées avec la méthode proposée. Fraction volume de fibres = 0,475. Pointillés : réponses de 10 configurations aléatoires (fibres circulaires de rayons identiques dont les centres sont tirés aléatoirement). F : fibres. M : matrice. AR : moyenne des réponses des configurations aléatoires. S0 (S45): réponse d'une cellule carrée contenant une fibre unique soumise à une traction simple à 0° (resp. 45°) par rapport à Ox. H0 et H45 : idem pour une cellule hexagonale. (a) matrice à écrouissage linéaire. (b) matrice parfaitement plastique.*

between the extreme responses of the square array (see *fig. 2 a*). At the local level, the plots of plastic strains indicate that the random arrangement of fibers inhibits the formation of long range shear bands and therefore strengthens the composite. These results can be helpful to estimate the representativity of the calculations based on the square or hexagonal arrays. The dispersion in the response of the 10 random cells depends on the number of fibers included in the image. This dispersion diminishes when the number of fibers, and hence the resolution of the image for a given precision, increases.

Overall flow stress. – Similar observations can be made when the matrix is perfectly plastic (see *fig. 2 b*). The square array exhibits strong transverse anisotropy. The identical low flow stresses in the diagonal direction (45°) for the hexagonal and square arrays is due to the presence of a shear plane passing through the matrix in both configurations. The hexagonal array, although not rigorously isotropic, approaches transverse isotropy. Note that the average flow stress of the random configurations is accurately predicted by the response of the hexagonal cell under tension along the 0° direction.

3.3 *Advantages of the method.* – 1. The method makes direct use of an image and does not require meshing of the microstructure.

2. The method is iterative. The formation and inversion of a stiffness matrix, as required by the methods proposed by Dumontet (1983) and Gobbe *et al.* (1988) also using Fourier series expansions, is avoided. The proposed algorithm permits the use of Fast Fourier Transforms algorithms available under optimized forms in most scientific packages and can be easily implemented on vectorial or parallel computers. As an illustration, an elastic iteration on an image of 256×256 pixels (131,000 degrees of freedom) requires 0.3 sec. on one processor of a CRAY YMP2E, while a complete elastic-plastic analysis of a $1,024 \times 1,024$ image requires 1 hr. 40 min. for the case of a material with a linear-hardening matrix.

3. The incompressibility constraint, $\mathbf{div}\,(\mathbf{u}) = 0$, can be taken into account by the algorithm without modifications, because the tensor $\hat{\Gamma}^0_{ijkh}$ has a finite limit when λ^0 tends to $+\infty$.

4. The method can be easily extended to compute the overall conductivity of composites.

REFERENCES

H. DUMONTET, Homogénéisation par développements en séries de Fourier, *C. R. Acad. Sci. Paris*, 296, Series II, 1983, pp. 1625-1628.
C. GOBBE, J. GOUNOT and M. QUINTARD, Approche spectrale du calcul tridimensionnel de propriétés équivalentes d'un milieu hétérogène, *C. R. Acad. Sci. Paris*, 307, Series II, 1988, pp. 1687-1692.
E. KRONER, *Statistical Continuum Mechanics*, Springer Verlag, Wien 1972, p. 117.
J. C. MICHEL and P. SUQUET, On the strength of composite materials: variational bounds and computational aspects, *Topology Design of Structures*, M. P. BENDSOE and C. MOTA-SOARES Eds., Kluwer Pub., 1993, pp. 355-374.
T. NAKAMURA and S. SURESH, Effects of thermal residual stresses and fiber packing on deformation of metal-matrix composites, *Acta Metall. Mater.*, 41, 1993, pp. 1665-1681.
P. SUQUET, Une méthode simplifiée pour le calcul des propriétés élastiques de matériaux hétérogènes à structure périodique, *C. R. Acad. Sci. Paris*, 311, Series II, 1990, pp. 769-774.

Laboratoire de Mécanique et d'Acoustique,
31, chemin Joseph-Aiguier, 13402 Marseille Cedex 20, France.